

## Optical properties of gallium oxide thin films

M. Rebien<sup>a)</sup> and W. Henrion

Hahn-Meitner-Institut, Abteilung Silizium-Photovoltaik, Kekuléstr. 5, D-12489 Berlin, Germany

M. Hong and J. P. Mannaerts

Agere Systems, Electronic Devices Research Laboratory, Murray Hill, New Jersey 07974

M. Fleischer

Siemens AG, Corporate Technology, Otto-Hahn-Ring 6, D-81739 Munich, Germany

(Received 27 March 2002; accepted for publication 9 May 2002)

The optical functions of  $\beta$ -Ga<sub>2</sub>O<sub>3</sub> thin films have been determined by ellipsometry from 0.74–5 eV. Several electron-beam evaporated and rf magnetron sputtered films of different thicknesses were investigated using a multisample technique. Refractive index values comparable to those of bulk material are found. Cauchy dispersion model fits yield a high-frequency dielectric constant  $\epsilon_\infty$  of 3.57. Above 4.7 eV a direct absorption edge is observed. © 2002 American Institute of Physics. [DOI: 10.1063/1.1491613]

The stable oxide of gallium, monoclinic  $\beta$ -Ga<sub>2</sub>O<sub>3</sub>, is a wide band gap material.<sup>1,2</sup> While current applications include luminescent phosphors<sup>3</sup> and gas sensors<sup>4</sup> it has been recognized as a promising candidate for deep-ultraviolet transparent conductive oxides (deep-UV TCO).<sup>5–7</sup> In addition,  $\beta$ -Ga<sub>2</sub>O<sub>3</sub> may be applied in textured dielectric coatings for solar cells.<sup>8</sup> A value of the refractive index close to  $\sqrt{n_{\text{GaAs}}}$  allows the preparation of efficient single-layer antireflective coatings for GaAs. Renewed interest with respect to the passivation of GaAs surfaces arose in connection with the realization of a very low electronic interface state density using Ga<sub>2</sub>O<sub>3</sub>/Gd<sub>2</sub>O<sub>3</sub> mixed oxides.<sup>9</sup>

Accurate determination of the optical functions is an essential prerequisite for device simulations and gives the opportunity to improve material preparation. The anisotropic absorption edge of  $\beta$ -Ga<sub>2</sub>O<sub>3</sub> single crystals has been investigated thoroughly.<sup>1</sup> However, refractive index dispersion of high-quality material in the uv–visible–near infrared (UV–VIS–NIR) spectral range has not been reported. Published refractive index data<sup>10</sup> are either restricted to a single spectral position<sup>11–13</sup> or have been determined on material with a high density of structural defects.<sup>14</sup>

Here we report the linear optical properties of electron-beam deposited and sputtered  $\beta$ -Ga<sub>2</sub>O<sub>3</sub> thin films. A multi-sample analysis of ellipsometric spectra recorded at multiple angles of incidence was performed to extract the optical functions using appropriate layer models. A comparison is made between refractive index spectra of both types of films and the absorption edges are determined.

$\beta$ -Ga<sub>2</sub>O<sub>3</sub> films on GaAs were prepared by electron-beam evaporation of  $\beta$ -Ga<sub>2</sub>O<sub>3</sub> pellets at a growth rate of about 0.5 Å/s. According to transmission electron microscopy investigations the films consist of randomly distributed microcrystallites within an amorphous matrix.<sup>15</sup> The films were deposited onto an epitaxial GaAs buffer layer (Si doping density  $1.6 \times 10^{16} \text{ cm}^{-3}$ ) on (001)-oriented GaAs substrate wafers (Si doping density  $2 \times 10^{18} \text{ cm}^{-3}$ ). Details can

be found in Ref. 15. Furthermore,  $\beta$ -Ga<sub>2</sub>O<sub>3</sub> films were deposited on Si(001) by pseudoreactive sputter deposition employing a  $\beta$ -Ga<sub>2</sub>O<sub>3</sub> ceramic target in a magnetron configuration with 14 vol% oxygen added to the sputtering gas argon to avoid an oxygen deficit in the films. According to Rutherford backscattering measurements these films are of stoichiometric composition. X-ray diffraction revealed a nanocrystalline morphology with a crystallite size of  $\leq 10 \text{ nm}$ .<sup>16</sup>

Spectral ellipsometry (SE) measurements from 0.74 to 5 eV in 0.02 eV steps were carried out on a J.A. Woollam Co. VASE rotating analyzer ellipsometer at multiple angles of incidence of 56°, 66°, and 76° with an accuracy of 0.02°. The polarizer was tracked with the measured ellipsometric angle  $\Psi$ . Measurements at positive and negative polarizer angles were averaged. An automatic retarder allowed accurate determination of the difference of phase shifts  $\Delta$  over the whole

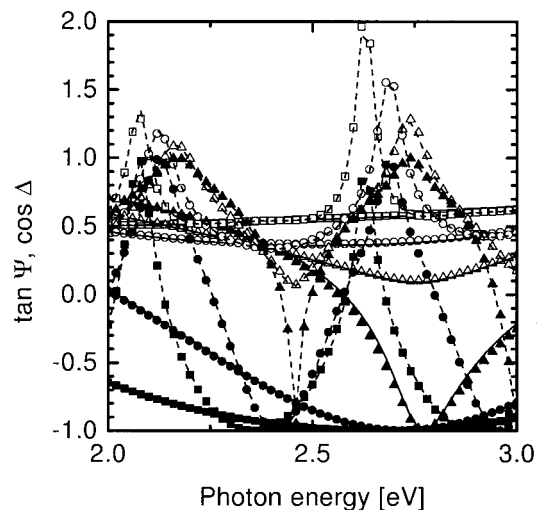


FIG. 1. Measured ellipsometric spectra of sputtered  $\beta$ -Ga<sub>2</sub>O<sub>3</sub> compared with a simultaneous fit of three samples (3–5, Table I). For better visibility only the measurements and fits of sample 3 (full line) and sample 4 (dashed line) in a limited spectral range are shown. The  $\tan \Psi$  (open symbols) and  $\cos \Delta$  (filled symbols) spectra were taken at three angles of incidence 56° (squares), 66° (circles), and 76° (triangles).

<sup>a)</sup>Electronic mail: rebien@hmi.de

TABLE I. Investigated samples and thickness values determined in multisample fits. The surface roughness of the sputtered films ( $\approx 1$  nm) was highly correlated to the thickness ( $\approx 3$  nm) of the interfacial  $\text{SiO}_2$ . This interdependence, however, did not significantly affect the other fit parameters. 90% confidence limits are also given.

| Sample number | Deposition method         | Substrate | Film thickness (nm) | Max thickness inhomogeneity | Surface roughness (nm) |
|---------------|---------------------------|-----------|---------------------|-----------------------------|------------------------|
| 1             | Electron-beam evaporation | GaAs      | $31.9 \pm 0.1$      | 9%                          | $2.8 \pm 0.1$          |
| 2             | Electron-beam evaporation | GaAs      | $58.95 \pm 0.07$    | 4.8%                        | $3.8 \pm 0.1$          |
| 3             | Sputtering                | Si        | $127.7 \pm 0.2$     | 3%                          | ...                    |
| 4             | Sputtering                | Si        | $597.5 \pm 0.2$     | 0.9%                        | ...                    |
| 5             | Sputtering                | Si        | $2468 \pm 0.6$      | 0.45%                       | ...                    |

range of  $0^\circ$ – $360^\circ$  and of partial depolarization.<sup>17</sup> For comparison, near-normal hemispherical reflectance (R) from 0.5 to 6.2 eV was measured using a conventional double-beam spectrophotometer equipped with an integrating sphere. All measurements were performed at room temperature.

Standard SE<sup>18</sup> determines the ratio of diagonal reflection Jones matrix elements  $r_{pp}/r_{ss} = \tan \Psi \cdot \exp(i\Delta)$ , where  $r_{pp}$  ( $r_{ss}$ ) is the complex Fresnel reflection coefficient parallel (perpendicular) to the plane of incidence.  $\Psi$  and  $\Delta$  are the ellipsometric angles reported here as  $\tan \Psi$  and  $\cos \Delta$ .

A model-based regression analysis using an error function weighted to the experimental error allows to extract the complex refractive index  $n + ik$  ( $n$ : refractive index,  $k$ : extinction coefficient) as well as film thickness and surface roughness.<sup>19</sup> The accuracy of data deduced from a layer model based analysis critically depends both on model quality and on accuracy of the substrate optical functions. The  $\beta$ - $\text{Ga}_2\text{O}_3$  films were modelled as a rough homogeneous layer on a semi-infinite substrate. For films on silicon the native  $\text{SiO}_2$  interlayer was included in the model. Surface roughness on a scale much smaller than the light wavelength was approximated by a Bruggeman effective medium layer consisting of 50% voids and 50% of the  $\beta$ - $\text{Ga}_2\text{O}_3$  underneath.<sup>20</sup> Concerning GaAs optical functions, available datasets for doped GaAs are not sufficiently accurate. Therefore, we used the dataset of Zollner for intrinsic GaAs.<sup>21</sup> While these comprise the best representation of the atomi-

cally smooth substrate surface, near the interband critical points errors are introduced which can, however, be neglected if a dispersion model fit is performed in a wide spectral range. The uncertainty in optical functions of the doped GaAs wafer precluded the  $\beta$ - $\text{Ga}_2\text{O}_3$  refractive index determination below a photon energy of 1.5 eV, where the buffer layer becomes transparent. Silicon and fused  $\text{SiO}_2$  optical functions were taken from Refs. 22 and 23, respectively. The ambient refractive index is approximated with  $n = 1$ .

For each type of preparation samples of significantly different film thickness were modelled simultaneously in a multisample approach.<sup>23</sup> Three sputter deposited samples and two electron-beam evaporated samples, respectively, were selected to ensure minimum film property variations with thickness. First, a Cauchy dispersion model for the refractive index  $n = n_\infty + B/\lambda^2 + C/\lambda^4$  (Ref. 24) was employed in the film transparency range to deduce film thickness, roughness values, and refractive index dispersion. Cauchy dispersion model parameters and in the case of Si substrates the  $\text{SiO}_2$  interlayer thickness were coupled during the multisample fits. Film thickness and surface roughness were allowed to vary for each sample. The investigated films together with their thickness are compiled in Table I. Then, spectral point-by-point fits were performed to extract both  $n$  and  $k$  at each spectral position. The good agreement between both  $n$  spectra provides a first check of the model. As an example, Fig. 1 shows part of the experimental spectra together with a simultaneous fit using the same model with different  $\beta$ - $\text{Ga}_2\text{O}_3$

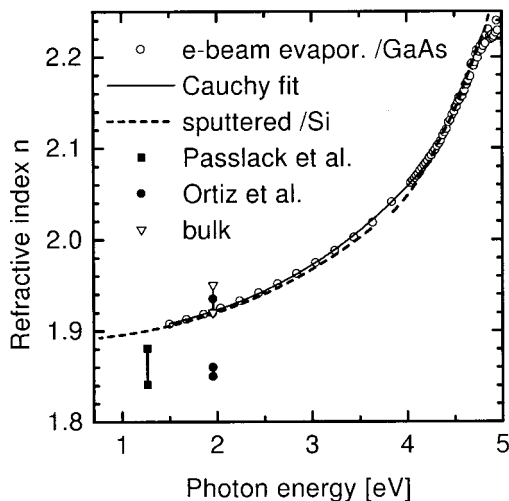


FIG. 2. Refractive index spectra derived from the multisample fits. Cauchy dispersion model parameters are given in Table II. Refractive index ranges from literature are included for electron-beam deposited films (see Ref. 11), as sprayed and annealed thin films (see Ref. 12) as well as bulk material (see Ref. 13).

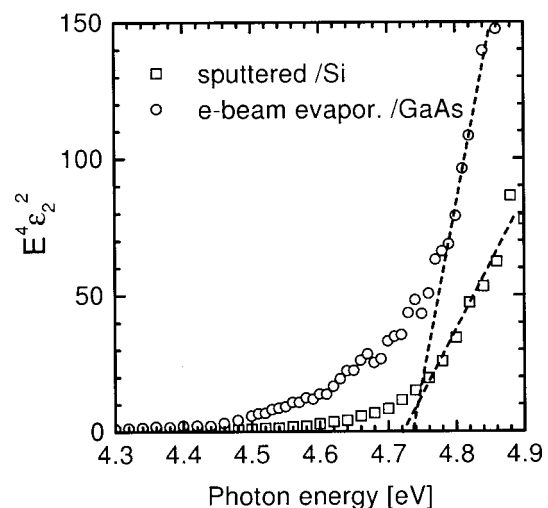


FIG. 3. Imaginary part of the dielectric function  $\epsilon_2 = 2nk$  in the plot for direct allowed transitions. Linear extrapolation to determine the direct band gap is indicated by dashed lines.

TABLE II. Cauchy model parameters of refractive index dispersion  $n = n_{\infty} + B/\lambda^2 + C/\lambda^4$  ( $\lambda$  in  $\mu\text{m}$ ) of  $\beta\text{-Ga}_2\text{O}_3$  films extracted from multisample fits of the ellipsometric spectra.

| Deposition method         | spectral range ( $\mu\text{m}$ ) | $n_{\infty}$        | B ( $\mu\text{m}^2$ ) | C ( $\mu\text{m}^4$ )   |
|---------------------------|----------------------------------|---------------------|-----------------------|-------------------------|
| Electron-beam evaporation | 0.295–0.826 (1.5–4.2 eV)         | $1.891 \pm 0.002$   | $0.0110 \pm 0.0005$   | $0.00048 \pm 0.00004$   |
| Sputtering                | 0.342–1.630 (0.76–3.62 eV)       | $1.8883 \pm 0.0003$ | $0.01140 \pm 0.00007$ | $0.000359 \pm 0.000007$ |

film thicknesses. Fit parameter correlation was found to be generally small. Only the surface roughness of the sputtered films was strongly correlated to the thickness of the interfacial  $\text{SiO}_2$  (Table I). Depolarization spectra (not shown) were fitted equally well.<sup>25</sup> The rough sample backside suppressed specular incoherent reflections leaving film thickness non-homogeneity and spectral bandwidth as possible causes of sizeable depolarization for the highly specularly reflecting films under investigation.<sup>26</sup> The influence of the spectral bandwidth set by the monochromator was small compared to film thickness variations. Depending on the measurement spot size, which is a function of the angle of incidence, different values of depolarization have been observed. Hence, the thickness non-homogeneity values were fitted separately for each angle of incidence. The maximum values are given in Table I. The use of more complicated layer models leads to strong fit parameter correlations and does not significantly improve the fit. Further confirmation for the modelling is indicated by a good agreement between measured reflectance spectra and those calculated using the film optical functions determined ellipsometrically.<sup>25</sup>

In Fig. 2 the resulting refractive index spectra are shown together with comprehensive values from literature. Even for the two very different preparation methods and substrates as well as the wide range of film thickness of the investigated samples, the resulting dispersion curves are nearly identical. As a maximum error for the  $\beta\text{-Ga}_2\text{O}_3$  refractive index the maximum difference between both curves of 0.02 near 3.8 eV can be taken, although the measurement and modelling errors are smaller. This deviation is attributed to small variations between different deposition methods and runs, differences in film morphology, or small inhomogeneity within the films. A high-frequency dielectric constant  $\epsilon_{\infty}$  of 3.57 (corresponding to  $n_{\infty} = 1.89$ ) was deduced from the Cauchy model fits (Table II). Absolute  $n$  values in the range of bulk material indicate a compact nature of the films. No clear signs of refractive index anisotropy were observed. For the determination of the anisotropic optical functions of this monoclinic material the investigation of high-quality single crystals is required.

Absorption in the films is below the detection level in most of the spectral range investigated. The direct absorption edge (Ref. 27) was obtained from the imaginary part of the dielectric function  $\epsilon_2 = 2nk$  (Fig. 3). The values of 4.72 eV (sputtered  $\beta\text{-Ga}_2\text{O}_3$ ) and 4.74 eV (e-beam evaporated  $\beta\text{-Ga}_2\text{O}_3$ ) are close to that of single crystals with E||b light polarization.<sup>1</sup> Small absorption below this value and a likely lower edge around 4.5 eV as reported in Refs. 1 and 14 cannot unambiguously be distinguished from layer model inaccuracies. The comparatively larger absorption of the electron-beam evaporated material above 4.5 eV compared to the sputtered films is attributed to inaccurate representa-

tion of the substrate optical functions in particular near the GaAs interband critical points where deviations from the ideally smooth interface have the most pronounced effect. Likewise for pulsed laser deposited films small absorption values were observed below the direct absorption edge of 4.9 eV.<sup>7</sup>

In conclusion, we have reported the linear optical functions of thin film  $\beta\text{-Ga}_2\text{O}_3$  in the UV–VIS–NIR spectral range. Good agreement was found for two different preparation techniques.

<sup>1</sup>N. Ueda, H. Hosono, R. Waseda, and H. Kawazoe, Appl. Phys. Lett. **71**, 933 (1997).

<sup>2</sup>J. Åhman, G. Svensson, and J. Albertsson, Acta Crystallogr., Sect. C: Cryst. Struct. Commun. **52**, 1336 (1996).

<sup>3</sup>T. Minami, T. Nakatani, and T. Miyata, J. Vac. Sci. Technol. A **18**, 1234 (2000).

<sup>4</sup>J. Frank, M. Fleischer, H. Meixner, and A. Feltz, Sens. Actuators B **49**, 110 (1998).

<sup>5</sup>T. J. Coutts, D. L. Young, and X. Li, MRS Bull. **25**, 58 (2000).

<sup>6</sup>N. Ueda, H. Hosono, R. Waseda, and H. Kawazoe, Appl. Phys. Lett. **70**, 3561 (1997).

<sup>7</sup>M. Orita, H. Ohta, M. Hirano, and H. Hosono, Appl. Phys. Lett. **77**, 4166 (2000).

<sup>8</sup>J. M. Gee, H. L. Tardy, T. D. Hund, R. Gordon, and H. Liang, in *Proceedings of the 24th IEEE Photovoltaics Specialist Conference*, 1994, p. 1274.

<sup>9</sup>M. Hong, Z. H. Lu, J. Kwo, A. R. Kortan, J. P. Mannaerts, J. J. Krajewski, K. C. Hsieh, L. J. Chou, and K. Y. Cheng, Appl. Phys. Lett. **76**, 312 (2000).

<sup>10</sup>D. F. Edwards, in *Handbook of Optical Constants of Solids III*, edited by E. D. Palik (Academic, Orlando, 1998), pp. 753–760, and references therein.

<sup>11</sup>M. Passlack, E. F. Schubert, W. S. Hobson, M. Hong, N. Moriya, S. N. G. Chu, K. Konstadinidis, J. P. Mannaerts, M. L. Schnoes, and G. J. Zydzik, J. Appl. Phys. **77**, 686 (1995).

<sup>12</sup>A. Ortiz, J. C. Alonson, E. Andrade, and C. Urbiola, J. Electrochem. Soc. **148**, F26 (2001).

<sup>13</sup>*CRC Handbook of Chemistry and Physics*, 70th ed., edited by R. C. Weast (CRC, Boca Raton, 1989), p. B-92.

<sup>14</sup>T. Matsumoto, M. Aoki, A. Kinoshita, and T. Aono, Jpn. J. Appl. Phys. **13**, 737 (1974).

<sup>15</sup>M. Hong, M. A. Marcus, J. Kwo, J. P. Mannaerts, A. M. Sergent, L. J. Chou, K. C. Hsieh, and K. Y. Cheng, J. Vac. Sci. Technol. B **16**, 1395 (1998).

<sup>16</sup>M. Fleischer and H. Meixner, J. Mater. Sci. Lett. **11**, 1728 (1992).

<sup>17</sup>B. Johs, J. A. Woollam, C. M. Herzinger, J. Hilfiker, R. Synowicky, and C. L. Bungay, SPIE Crit. Rev. Opt. Sci. Technol. **CR72**, 29 (1999).

<sup>18</sup>R. M. A. Azzam and N. M. Bashara, *Ellipsometry and Polarized Light* (Elsevier, Amsterdam, 1987).

<sup>19</sup>C. M. Herzinger, P. G. Snyder, B. Johs, and J. A. Woollam, J. Appl. Phys. **77**, 1715 (1995).

<sup>20</sup>G. E. Jellison, Jr., Thin Solid Films **234**, 416 (1993).

<sup>21</sup>S. Zollner, J. Appl. Phys. **90**, 515 (2001).

<sup>22</sup>B. Brixner, in *Handbook of Optical Constants of Solids*, edited by E. D. Palik (Academic, Orlando, 1985), pp. 759–760.

<sup>23</sup>C. M. Herzinger, B. Johs, W. A. McGahan, J. A. Woollam, and W. Paulson, J. Appl. Phys. **83**, 3323 (1998).

<sup>24</sup>D. Y. Smith, M. Inokuti, and W. Karstens, J. Phys.: Condens. Matter **13**, 3883 (2001).

<sup>25</sup>M. Rebien, Ph.D. thesis, to be published.

<sup>26</sup>A. Röseler, J. Opt. Soc. Am. A **9**, 1124 (1992).

<sup>27</sup>P. Y. Yu and M. Cardona, *Fundamentals of Semiconductors*, 3rd ed. (Springer, Berlin, 2001), p. 259.